Interplay between quantum Zeno and anti-Zeno effects in a nondegenerate hyper-Raman nonlinear optical coupler

Moumita Das,[1] Kishore Thapliyal,[2,*] Biswajit Sen,[3,†] Jan Peřina,[4] and Anirban Pathak[5,‡]

[1]*Department of Physics, Siliguri College, Siliguri 734 001, India*

[2]*RCPTM, Joint Laboratory of Optics of Palacky University and Institute of Physics of Academy of Science of the Czech Republic, Faculty of Science, Palacky University, 17 listopadu 12, 771 46 Olomouc, Czech Republic*

[3]*Department of Physics, Vidyasagar Teachers' Training College, Midnapore 721 101, India*

[4]*Joint Laboratory of Optics of Palacky University and Institute of Physics of Academy of Science of the Czech Republic, Faculty of Science, Palacky University, 17 listopadu 12, 771 46 Olomouc, Czech Republic*

[5]*Jaypee Institute of Information Technology, A-10, Sector 62, Noida UP 201309, India*

(Received 23 May 2020; accepted 21 December 2020; published 11 January 2021)

Quantum Zeno and anti-Zeno effects are studied in an asymmetric nonlinear optical coupler composed of a probe waveguide and a system waveguide. The system is a nonlinear waveguide operating under the nondegenerate hyper-Raman process, while both the pump modes in the system are constantly interacting with the probe waveguide. The effect of the presence of the probe on the spatial evolution of the system in terms of the number of photons in Stokes and anti-Stokes modes as well as the phonon number is quantified as the Zeno parameter. The negative (positive) values of the Zeno parameter in the specific mode are considered as the signatures of the quantum Zeno (anti-Zeno) effect in that mode of the system. It is observed that the initial phase difference between all the coherent amplitudes involved in the Stokes and anti-Stokes generation processes can be controlled to induce a transition between quantum Zeno and anti-Zeno effects for the hyper-Raman process in both cases with and without phase matching. However, in the case of the hyper-Raman process in the system waveguide without a phase matching, the phase mismatch parameters, due to difference in the wave vectors of all the modes involved in the Stokes and anti-Stokes generation processes, can also be used analogously to cause the desired crossover. Further, the general nature of the physical system and the perturbative technique used here allow us to analytically study the possibilities of observing quantum Zeno and anti-Zeno effects in a large number of special cases, including situations where the process is spontaneous or partially spontaneous and/or the system is operated under a degenerate hyper-Raman process, or a simple Raman process.

DOI: 10.1103/PhysRevA.103.013713

I. INTRODUCTION

The response of a quantum system to a measuring device can not only distinctively distinguish a quantum system from a classical system; it also plays an extremely important role in the subsequent evolution of the system. Interestingly, sufficiently frequent interactions can even suppress the time evolution. This phenomenon of suppressing (inhibition of) the time evolution of a quantum system by frequent interaction is known as the quantum Zeno effect (QZE) [1]. It was introduced by Mishra and Sudarshan in 1977 [1], in an interesting work, where they showed that if an unstable particle is continuously measured, it will never decay. They realized that this situation is analogous to one of the well-known Zeno's paradoxes, which were introduced by the Greek philosopher Zeno of Elea in the 5th century BC and which have persistently fascinated scientists and philosophers since then. Considering the analogy, Mishra and Sudarshan referred to the quantum phenomenon analogous to the classical Zeno's paradox as *Zeno's paradox in quantum theory*. This led to the formal origin of QZE, but the quantum analog of Zeno's paradox was also studied before the work of Mishra and Sudarshan [1]. Specifically, Khalfin had studied nonexponential decay of unstable atoms [2] in the late 1950s and early 1960s.

Interestingly, it was soon recognized that measurement can also lead to a phenomenon which can be viewed as the inverse of QZE. In such a phenomenon, continuous measurement (or interaction) leads to the enhancement of the evolution instead of the inhibition (see Refs. [3–8]) and is referred to as the quantum anti-Zeno effect (QAZE) or inverse Zeno effect. Interestingly, QZE and QAZE are known to be evinced through various equivalent ways [9]. For the present work, a particularly relevant manifestation of QZE would be one in which QZE or QAZE is viewed as a process led by continuous interaction between a system and a probe [4]. Specifically, Kraus used the continuous interaction with an external agent as "watchdog effect" [10] which was later shown quantitatively related to the QZE by pulsed measurement [11]. Along the same line, studies of the open quantum system, i.e., a continuous interaction between a quantum system and ambient environment, led to unification of dynamical

*kishore.thapliyal@upol.cz
†bsen75@yahoo.co.in
‡anirban.pathak@jiit.ac.in

decoupling with QZE [12] and found that the presence of QZE or QAZE is decided by the parameters of the reservoir [13]. Specifically, in what follows, we aim to study the continuous interaction-type manifestation of QZE in hyper-Raman processes, where it will be considered that a nonlinear waveguide is operating under a nondegenerate hyper-Raman process and is continuously interacting with a probe waveguide. A change in the dynamics of the nonlinear system waveguide due to the presence of the probe waveguide is quantified as increase or decrease in the photon numbers of Stokes and anti-Stokes modes as well as the phonon number. Thus, QZE or QAZE in the present scenario will lead to suppression or enhancement of hyper-Raman scattering due to continuous observation by an external probe. This is expected to reveal the origin of nonclassical features in the hyper-Raman scattering and help us to analyze whether generation of nonclassical states can be controlled by using an auxiliary probe. Earlier, QZE has been reported by some of the present authors in Raman processes [14], an asymmetric and a symmetric nonlinear optical coupler [6,8], and a parity-time symmetric linear optical coupler [7]. However, it has never been studied in the systems involving the hyper-Raman process due to its intrinsic mathematical difficulty.

Apart from the Raman process, QZE and QAZE have already been studied in various optical systems, like various types of optical couplers [6,14–17], parametric down-conversion [17–19], parametric down-conversion with losses [20], and an arrangement of beam splitters [21]. In these studies on QZE in optical systems, often the pump mode was considered strong, and thus the complexity of a completely quantum mechanical treatment has been circumvented. Keeping this in mind, here we plan to use a completely quantum mechanical description of the nonlinear optical coupler composed of a probe and a nonlinear waveguide operating under the hyper-Raman process. We have considered a general Raman process here, namely the nondegenerate hyper-Raman process, which allows us to reduce the corresponding results for Raman and degenerate hyper-Raman processes. The system of our interest, namely the nonlinear optical coupler, is easily realizable using photonic crystals and optical fibers [22–24]. Specifically, two waveguides, forming the directional coupler, interact through evanescent waves which allows us to control the interaction strength between them by regulating the interaction length (see [23,24] for details).

For about two decades, since the pioneering work of Mishra and Sudarshan, QZE remained as a problem of theoretical interest without any practical applications. The scenario started changing from the beginning of the 1990s as it became possible to experimentally realize QZE using different routes [25–27]. This enhanced the interest on QZE and that in turn led to many new proposals for applications of QZE [25,28–31]. For example, applications of QZE were proposed for the enhancement of the resolution of absorption tomography [30,31], reduction of communication complexity [32], and combating decoherence by confining dynamics in decoherence-free subspace [33]. Further, proposals for quantum interrogation measurement [25] and a counterfactual direct quantum communication protocol [29,34] using QZE have garnered much attention. Efforts have also been made to investigate QZE in the macroscopic world for large black holes [35] and in nonlinear waveguides in the context of stationary flows with localized dissipation [36]. Inspired by these applications of QZE, the general nature of the nonlinear (nondegenerate hyper-Raman) process under consideration, and availability of nonlinear optical couplers in integrated optics and optical fibers [37,38], here we study the possibility of QZE and QAZE using a completely quantum treatment in an asymmetric nonlinear optical coupler.

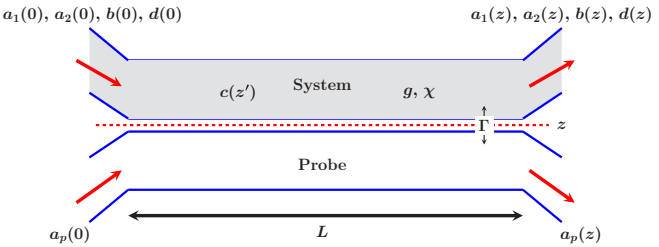

FIG. 1. Schematic diagram of an optical coupler of length L composed of a system waveguide, operating under a nondegenerate hyper-Raman process, interacting with a probe. The coupling coefficients as well as optical (namely, probe a_p, nondegenerate hyper-Raman pump a_1, a_2, Stokes b, and anti-Stokes d) and phonon (c) modes are indicated in the diagram.

Using a perturbative technique (known as the Sen-Mandal technique [24,39–41]) for obtaining an operator solution of Heisenberg's equations of motion, we have obtained closed-form analytic expressions for the spatial evolution of the relevant field operators present in the system momentum operator that provides a completely quantum mechanical description of the nonlinear optical coupler composed of the probe and a nonlinear waveguide operating under the hyper-Raman process. It is well established that this method produces better results compared to the conventional short-length approach [24,39–41] as the present solution is not restricted by length or time. In what follows, we will see that the use of this perturbative technique has revealed compact analytic expressions for the Zeno parameter which clearly illustrate that in the system under consideration (and in many special cases of it), it is possible to observe QZE and QAZE in Stokes, anti-Stokes, and phonon modes for the suitable choices of system parameters. Further, it will be shown that phase difference and mismatch parameters can be controlled to execute a crossover between QZE and QAZE.

The rest of the paper is organized as follows. In Sec. II, we briefly describe the hyper-Raman process based on the asymmetric nonlinear optical coupler system of our interest. Subsequently, we report the expressions of the Zeno parameter for both photon and phonon modes in the system in Sec. III. A detailed discussion of the obtained results is summarized in Sec. IV. Finally, the paper is concluded in Sec. V.

II. PHYSICAL SYSTEM

The physical system of our interest is actually a codirectional asymmetric nonlinear optical coupler composed of a probe and a system, which is a nonlinear waveguide operating under the hyper-Raman process (see Fig. 1 for a schematic diagram). The momentum operator of the complete

(probe+system) physical system is given by

$$\begin{aligned} G &= G_{\text{probe}} + G_{\text{system}} + G_{\text{Int}}: \\ G_{\text{probe}} &= k_p a_p^\dagger a_p, \\ G_{\text{system}} &= k_{a_1} a_1^\dagger a_1 + k_{a_2} a_2^\dagger a_2 + k_b b^\dagger b + k_c c^\dagger c + k_d d^\dagger d \\ &\quad + (g a_1 a_2 b^\dagger c^\dagger + \chi a_1 a_2 c d^\dagger + \text{H.c.}), \\ G_{\text{Int}} &= \Gamma a_p a_1^\dagger a_2^\dagger + \text{H.c.}, \end{aligned} \tag{1}$$

where $\hbar = 1$ (the same convention is used in the rest of the paper), and H.c. stands for the Hermitian conjugate. The annihilation (creation) operators $a_p(a_p^\dagger)$, $a_i(a_i^\dagger)$, $b(b^\dagger)$, $c(c^\dagger)$, and $d(d^\dagger)$ correspond to the probe pump (indexed by subscript p), nondegenerate hyper-Raman laser (this is also a pump, but it is indexed by subscript $i = 1, 2$ to distinguish from the probe pump), Stokes, vibration (phonon), and anti-Stokes modes, respectively. All the field operators introduced here obey the usual bosonic commutation relation. Wave vectors corresponding to the probe, pump 1 and 2, Stokes, phonon, and anti-Stokes modes are denoted by k_p, k_{a_1}, k_{a_2}, k_b, k_c, and k_d, respectively. The Stokes and anti-Stokes coupling constants are described by parameters g and χ, respectively. Further, Γ denotes the interaction constant between the probe and the two pump modes present in the hyper-Raman process in the system. The probe interacts with the system waveguide continuously through the evanescent waves. Following the continuous observation analog of QZE [4], we can describe $G = G_{\text{system}} + G_{\text{measurement}}$ where $G_{\text{measurement}} = G_{\text{probe}} + G_{\text{Int}}$, and by controlling the coupling strength Γ we can tune the effect of the probe mode on the reduced dynamics of the hyper-Raman waveguide. Notice that the probe mode interacts with non-degenerate pump modes of the system waveguide only unlike [14] where the probe interacts either with the Stokes or anti-Stokes mode. This allows us to observe QZE and QAZE in both Stokes and anti-Stokes modes simultaneously which was not permitted in the framework of [14].

We obtain the Heisenberg equations of motion for the momentum operator (1) of the system of interest, which gives us six coupled differential equations for the six bosonic operators present in the expression of the momentum operator. To obtain the spatial evolution of all the operators we use Sen-Mandal perturbative technique as dimensionless quantities gz, χz, and Γz are small compared to unity. In Appendix A, we have reported Heisenberg's equations of motion and spatial evolution of the relevant number operators for the Stokes, anti-Stokes, and phonon modes using the Sen-Mandal technique. Mathematical details of the perturbative solution are given in Appendix B. Further, it is worth stressing that we neglect the losses in the nondegenerate hyper-Raman waveguide system considering a one-passage arrangement [14], while inclusion of the damping terms is expected to reduce the quantum effects only.

In the next section, we will show that the obtained number operators would provide us analytic expressions of the Zeno parameter for the respective modes. The general nature of the solution and the process under consideration allow us to deduce the results for Raman and degenerate hyper-Raman processes as well as the corresponding short-length solution in the limiting cases. Further, the present solution inherently introduces phase mismatch parameters in the Stokes and anti-Stokes generation, and thus provides the solution for a set of Raman processes in both cases with and without phase matching.

III. QUANTUM ZENO AND ANTI-ZENO EFFECTS

In order to investigate the QZE and QAZE in a hyper-Raman active medium, we consider the initial composite coherent state $|\psi(0)\rangle$ as the product of the initial coherent states of the probe, pump, Stokes, phonon, and anti-Stokes modes as $|\alpha\rangle$, $|\alpha_j\rangle$, $|\beta\rangle$, $|\gamma\rangle$, and $|\delta\rangle$, respectively. Hence, the initial state is considered to be

$$|\psi(0)\rangle = |\alpha\rangle \otimes |\alpha_1\rangle \otimes |\alpha_2\rangle \otimes |\beta\rangle \otimes |\gamma\rangle \otimes |\delta\rangle, \tag{2}$$

and the field operator a_p operating on the initial state gives

$$a_p(0)|\psi(0)\rangle = \alpha|\psi(0)\rangle, \tag{3}$$

where $\alpha = |\alpha|e^{i\varphi_p}$ is the complex eigenvalue with $|\alpha|^2$ initial mean number of photons and φ_p phase angle in the probe mode a. In a similar manner, coherent state parameters for all the optical and phonon modes involved in the hyper-Raman process can be defined as $\Lambda_j = |\Lambda_j|e^{i\varphi_j}$ for complex amplitudes $\Lambda_j : \Lambda \in \{\alpha, \beta, \gamma, \delta\}$ and corresponding phase angle φ_j with $j \in \{1, 2, b, c, d\}$ for the nondegenerate pump 1 and pump 2, Stokes, phonon, and anti-Stokes modes, respectively.

To quantify the role of the external probe in controlling the dynamics of hyper-Raman scattering we use the Zeno parameter [6–8] introduced as the difference of photon or phonon numbers in the presence and absence of the probe. We define the Zeno parameter as [6–8]

$$Z_i = \langle N_i \rangle - \langle N_i \rangle_{\Gamma=0}, \tag{4}$$

where $i \in \{b, c, d\}$ and $N_i = i^\dagger i$ is the number operator. The conditions $Z_i < 0$ and $Z_i > 0$ correspond to the occurrence of QZE and QAZE in ith mode. Clearly, the negative (positive) values of the Zeno parameter represent that the number of photons or phonons in the system waveguide (i.e., $\langle N_i \rangle$) decreases (increases) from that in the absence of the probe waveguide (i.e., $\langle N_i \rangle_{\Gamma=0}$). We have reported the dynamics of number operators for Stokes, anti-Stokes, and phonon modes in Appendix A.

In what follows, we report the Zeno parameters for Stokes, anti-Stokes, and phonon modes obtained using these expressions.

To begin with, using Eq. (A2) in Eq. (4), the Zeno parameter for the Stokes mode is computed as

$$\begin{aligned} Z_b = \mathcal{C}_b \Bigg\{ &\frac{\cos\theta_2}{\Delta k_S(\Delta k_D + \Delta k_S)} + \frac{\cos(\Delta k_S z + \Delta k_D z - \theta_2)}{\Delta k_D(\Delta k_D + \Delta k_S)} \\ &- \frac{\cos(\Delta k_S z - \theta_2)}{\Delta k_D \Delta k_S} \Bigg\}, \end{aligned} \tag{5}$$

where we have used the initial phase differences among the different modes involved in the probe-Stokes and probe–anti-Stokes interactions as $\theta_1 = (\varphi_d - \varphi_p - \varphi_c)$ and $\theta_2 = (\varphi_p - \varphi_b - \varphi_c)$, respectively. Also, we have $\mathcal{C}_b = 2\Gamma g(|\alpha_1|^2 + |\alpha_2|^2 + 1)|\alpha||\beta||\gamma|$. Similarly, we have introduced phase mismatch parameters in Stokes, anti-Stokes,

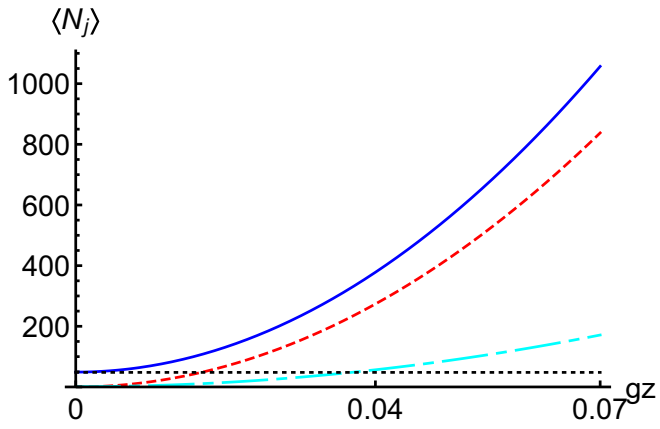

FIG. 2. Spatial evolution of the number of photons and phonons $\langle N_j\rangle \forall\, j \in \{b, d, c\}$ for Stokes, anti-Stokes, and phonon modes is shown in the smooth (blue), dashed (red), and dot-dashed (cyan) lines, respectively. The black dotted line corresponds to the constant of motion $\langle (N_b - N_d - N_c)\rangle$. We have chosen here the coupling coefficients $\chi = 1.2g$ and $\Gamma = 1.5g$ with initial coherent state amplitudes for all modes $\alpha = 9, \alpha_1 = 8.5, \alpha_2 = 8.3, \beta = 7, \gamma = 0.01, \delta = -1$. We have also used $\theta_j = 0$ and $\Delta k_S = 2 \times 10^{-2} g = 2\Delta k_A = 20\Delta k_D$. All the quantities shown here and in the rest of the plots are dimensionless.

and second-order coupling between the probe and system waveguides as $\Delta k_S = -k_{a_1} - k_{a_2} + k_b + k_c$, $\Delta k_A = k_{a_1} + k_{a_2} + k_c - k_d$, and $\Delta k_D = k_{a_1} + k_{a_2} - k_p$.

In a similar manner, the Zeno parameter for the anti-Stokes mode is computed using Eqs. (4) and (A4) and the following analytic expression is obtained:

$$Z_d = \mathcal{C}_d \left\{ \frac{\cos\theta_1}{\Delta k_A(\Delta k_A - \Delta k_D)} - \frac{\cos(\theta_1 + \Delta k_D z - \Delta k_A z)}{\Delta k_D(\Delta k_A - \Delta k_D)} + \frac{\cos(\theta_1 - \Delta k_A z)}{\Delta k_D \Delta k_A} \right\}, \tag{6}$$

where $\mathcal{C}_d = 2\Gamma\chi(|\alpha_1|^2 + |\alpha_2|^2 + 1)|\alpha||\gamma||\delta|$. The Zeno parameter for the phonon mode was also computed analytically using Eqs. (4) and (A3), but it was found that the same can be expressed as the difference of the other two Zeno parameters, i.e.,

$$Z_c = Z_b - Z_d. \tag{7}$$

This is a direct consequence of the conservation law: $[G, N_b - N_d - N_c] = 0$, and thus using this constant of motion [42] Eq. (7) follows. Apparently, this should be the case with degenerate hyper-Raman and Raman processes in the system, too, provided the probe-system interaction is with the pump mode; however, the probe-system interaction may be with the Stokes and anti-Stokes modes as in the case of earlier works [14].

For the sake of completeness, we have illustrated here spatial evolution of the number of Stokes and anti-Stokes photons as well as phonons in the nonlinear optical coupler in Fig. 2. We have explicitly shown that the quantity $\langle N_b - N_d - N_c\rangle$ remains constant during the evolution. Here and in what follows, the results obtained are mostly dependent on the relative dimensionless quantities.

IV. DISCUSSION

There are some interesting scenarios to consider for the present study, namely spontaneous, stimulated, and partially stimulated cases. These three cases are described depending upon the type of the Raman process undergoing in the system waveguide. Specifically, pump intensity is always nonzero $\alpha_i \neq 0$, while the Stokes, anti-Stokes, and phonon modes may be initially in vacuum or coherent states. Thus, we have with $S = \{\beta, \gamma, \delta\}$ the following:

(1) Spontaneous Raman process: $\mathcal{U} = 0\, \forall\, \mathcal{U} \in S$.

(2) Stimulated Raman process: $\mathcal{U} \neq 0\, \forall\, \mathcal{U} \in S$.

(3) Partially stimulated Raman process: $\mathcal{U} = 0$ and $\mathcal{V} \neq 0$ with $\mathcal{U} \in S$ and $\mathcal{V} \in S\backslash\mathcal{U}$.

Note that the probe mode has nonzero intensity initially in all cases, i.e., $\alpha \neq 0$, as otherwise QZE and QAZE cannot be observed. Specifically, from the expressions of $\mathcal{C}_j$, we can easily observe that in the spontaneous case, $Z_j = 0\, \forall\, j \in \{b, c, d\}$. Thus, neither QZE nor QAZE is observed in the spontaneous case. In other words, the presence of the probe does not affect the dynamics of boson numbers in the spontaneous hyper-Raman scattering in the validity of the perturbative solution. The stimulated case, i.e., when all the coherent modes are initially prepared with nonzero intensity, will be discussed in detail later. Prior to that, we may discuss the partially stimulated cases, where among Stokes, anti-Stokes, and phonon modes, initial intensity is nonzero for at most two modes and the same for other mode(s) is zero; of course, the pump modes have nonzero initial intensity. Consider a particular type of stimulated case, where $\beta \neq 0, \gamma \neq 0, \delta = 0$. In this case, we obtain $Z_d = 0 \neq Z_b = Z_c$, while with $\beta = 0, \gamma \neq 0, \delta \neq 0$ we obtain $Z_d = -Z_c \neq 0 = Z_b$. Thus, in the first type of partially stimulated case mentioned above, for a particular choice of phase difference and mismatch parameters, if we observe QZE (QAZE) in the Stokes mode, we will observe QZE (QAZE) in the phonon mode, too, but the anti-Stokes mode will not show any of the effects. Similarly, in the second type of partially stimulated case, for a particular choice of phase difference and mismatch parameters, if we observe QZE (QAZE) in the anti-Stokes mode, we will observe QAZE (QZE) in the phonon mode; the Stokes mode will not show any of the effects. The other possibility of a partially stimulated process with $\beta \neq 0, \gamma = 0, \delta \neq 0$ leads to a trivial case where $Z_j = 0\, \forall\, j \in \{b, c, d\}$ as $Z_j \propto |\gamma|$. There are a couple of other possibilities where two of the parameters β, γ, δ are simultaneously zero. It is easy to see that neither QZE nor QAZE will be observed in those cases. Specifically, for $\beta = 0, \gamma = 0, \delta \neq 0$ and $\beta \neq 0, \gamma = 0, \delta = 0$, we would not obtain QZE or QAZE in any mode as $\gamma = 0$ would ensure that $Z_j = 0\, \forall\, j \in \{b, c, d\}$. The same situation will arise in the case $\beta = 0, \gamma \neq 0, \delta = 0$ as $\mathcal{C}_j$ will vanish $\forall\, j \in \{b, c, d\}$. On the other hand, if the probe interacts with the Stokes or anti-Stokes mode we may expect to observe QZE or QAZE with the phonon vacuum in analogy to that in the Raman coupler [14].

From Eqs. (5) and (6), we can verify that $\mathcal{C}_j \propto 2\Gamma(|\alpha_1|^2 + |\alpha_2|^2 + 1)|\alpha||\gamma|\, \forall\, j \in \{b, c, d\}$ which is always

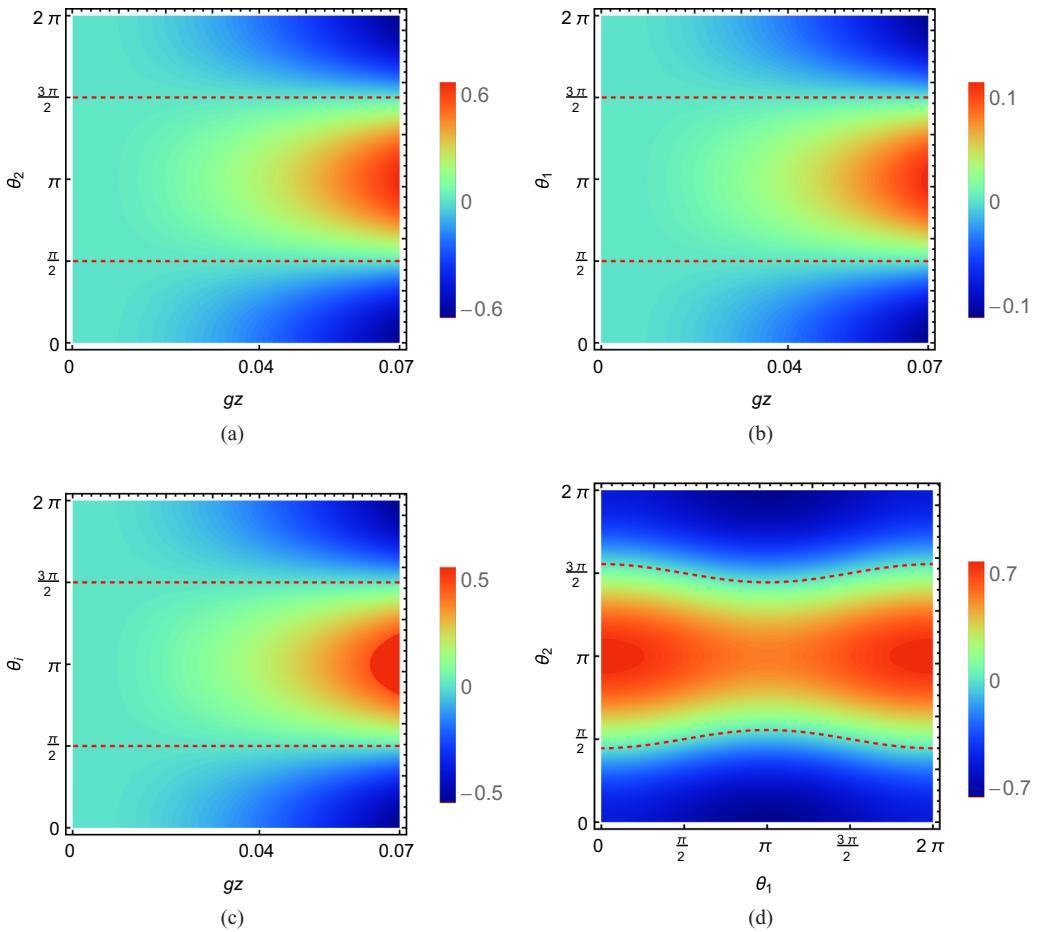

FIG. 3. Spatial evolution of Zeno parameter Z_j for (a) Stokes, (b) anti-Stokes, and (c)–(d) phonon modes as a function of the phase difference parameter θ_i. In (c), we have shown $Z_c(\theta_1 = \theta_2)$. We have also used $\Delta k_S = \Delta k_A = 10^{-2} g = 10\Delta k_D$. The rest of the parameters are the same as in the previous figure. The dashed (red) contour lines represent a crossover between QZE and QAZE.

positive and increases with coupling between the probe and system as well as the initial pump and probe intensities and the phonon numbers. Additionally, we can verify that $\mathcal{C}_b \propto g|\beta|$ and $\mathcal{C}_d \propto \chi|\delta|$. Thus, we can conclude that the coefficients $\mathcal{C}_j$ can only alter the depth of Zeno parameters by a scaling factor, but cannot induce a transition from QZE to QAZE or vice versa. Therefore, we can summarize that the occurrence of QZE or QAZE would depend only on the phase difference parameters and phase mismatches; i.e., we can safely restrict our discussion on the possibility of observing QZE and QAZE to a situation where the parametric dependence of the relevant Zeno parameters is viewed as $Z_b(Dk_D, Dk_S, \theta_2)$ and $Z_d(Dk_D, Dk_A, \theta_1)$. This analytic result helps us to clearly visualize the interplay between QZE and QAZE, and it also answers the following: What controls the dynamics of QZE and QAZE and which physical parameters may cause transition from one of them to the other? Before we discuss this further, it is worth discussing the behavior for the hyper-Raman system waveguide with phase matching.

Considering the phase-matching condition, that is, $\Delta k_D = \Delta k_S = \Delta k_A = 0$, we can obtain from Eqs. (5)–(7), in the limits of phase mismatches tending to zero, that

$$(Z_b)_{\mathrm{R}} = -\tfrac{1}{2}\mathcal{C}_b z^2 \cos\theta_2 \tag{8}$$

and

$$(Z_d)_{\mathrm{R}} = -\tfrac{1}{2}\mathcal{C}_d z^2 \cos\theta_1, \tag{9}$$

where R corresponds to the results with the phase-matching condition. Notice that phase difference parameters are significant in the presence of QZE and QAZE as $(Z_j)_{\mathrm{R}} \propto -\cos\theta_i$, while the depth of the Zeno parameters increases with $\mathcal{C}_j$ and propagation length z. We know that $\cos\theta_i > 0\,\forall\,\theta_i \in [0, \frac{\pi}{2}] \cup [\frac{3\pi}{2}, 2\pi]$ and $\cos\theta_i < 0\,\forall\,\theta_i \in [\frac{\pi}{2}, \frac{3\pi}{2}]$. Thus, QAZE (QZE) is observed in both Stokes and anti-Stokes modes when $\cos\theta_i$ is negative (positive). In this case, $(Z_c)_{\mathrm{R}} = -(\mathcal{C}_b \cos\theta_2 - \mathcal{C}_d \cos\theta_1) z^2$, which has dependence on both the phase difference parameters. If we consider $\theta_1 = \theta_2$, this will reduce to $(Z_c)_{\mathrm{R}}|_{\theta_1=\theta_2} = -(\mathcal{C}_b - \mathcal{C}_d) z^2 \cos\theta_i$, and thus, in this special case, QZE (QAZE) would be observed in the phonon mode if $\frac{g}{\chi} > \frac{|\delta|}{|\beta|}$ ($\frac{g}{\chi} < \frac{|\delta|}{|\beta|}$). Interestingly, most of the observations made here regarding phase difference parameters are also applicable in hyper-Raman case with small phase mismatches (cf. Fig. 3).

Consider a special case of the hyper-Raman process without phase matching in the system waveguide, when $\Delta k_D = \Delta k_S = -\Delta k_A$ in the support on the phonon mode as $\Delta k_S = -\Delta k_A$ ensures $2k_c = k_d - k_b$. In this case, Eqs. (5)–(7) can be

simplified to obtain

$$Z_j = -\frac{1}{2}\mathcal{C}_j z^2 \cos[\Delta k_D z + (-1)^i \theta_i]\mathrm{sinc}^2\left(\frac{\Delta k_D z}{2}\right), \quad (10)$$

where $i = 1$ for $j = d$ and $i = 2$ for $j = b$. It clearly shows that the general solution used here is modulated with the sinc function of the phase mismatch parameter [43,44]. Consequently, the present solution and the corresponding results are applicable to a relatively long length of the optical coupler in comparison to the corresponding short-length solution. Notice in Eq. (10) that $Z_j \propto \cos[\Delta k_D z + (-1)^j \theta_i]$, and thus a crossover between QZE and QAZE can be attained by controlling the phase mismatch $\Delta k_D z$. Therefore, if we assume the phase difference parameter $\theta_i = 0$, we can conclude that Z_j is negative (i.e., QZE is observed) only when $\Delta k_D z \in [0, \frac{\pi}{2}] \cup [\frac{3\pi}{2}, 2\pi]$; otherwise QAZE is observed.

To further stress this point, we have shown variation of the Zeno parameters with phase mismatch parameters in Fig. 4, where we can clearly see that a transition from QZE (QAZE) to QAZE (QZE) can be caused in both optical modes (phonon mode) for large values of phase mismatch after traversing sufficiently through the optical coupler. In all the plots, we have considered $\Delta k_S = \Delta k_A$ (unless stated otherwise) in the support on the pump mode as $2(k_{a_1} + k_{a_2}) = k_b + k_d$.

Taking into consideration both the phase mismatch parameters together (considering $\theta_j = 0$), a transition from QZE to QAZE in the Stokes mode can be induced for smaller values of the phase mismatch parameter than that shown in Fig. 4(a) by increasing the other phase mismatch parameter [shown in Fig. 5(a)]. In contrast, QZE for the anti-Stokes mode can be maintained for larger values of phase mismatch in anti-Stokes generation by increasing the value of phase mismatch between the pump modes of the system and probe waveguides [cf. Figs. 4(b) and 5(b)]. Similarly, QAZE can be made more dominant by increasing phase mismatch between the pump modes of the system and probe as shown in Fig. 5(c). Interestingly, phase mismatches in Stokes and anti-Stokes generation processes have starkly opposite effects on the Zeno parameter as the former increases it while the latter decreases it [cf. Fig. 5(d)].

Further extension of the present results with the phonon mode initially coherent to the chaotic phonon mode [43] gives that all the Zeno parameters become zero. Our results can also be used to deduce the presence of QZE and QAZE for degenerate hyper-Raman and Raman system waveguides from Eqs. (5)–(7) by considering $\alpha_2 = \alpha_1$ and $\alpha_2 = 0$, respectively. Therefore, we can conclude from the reduced results in those cases that the presence of QZE and QAZE in the parametric space will remain unchanged, though some changes in the depth of the Zeno parameter are expected due to changes in the scaling factors $\mathcal{C}_j$.

In view of the availability of on-chip Raman devices [45,46], photonics often used in quantum information experiments [22,23,37,38], a few attempts at hyper-Raman scattering [47,48], and the recent set of experiments exploiting Raman processes for quantum technology [49,50], we anticipate the current results would soon become verifiable for the set of Raman processes presented here.

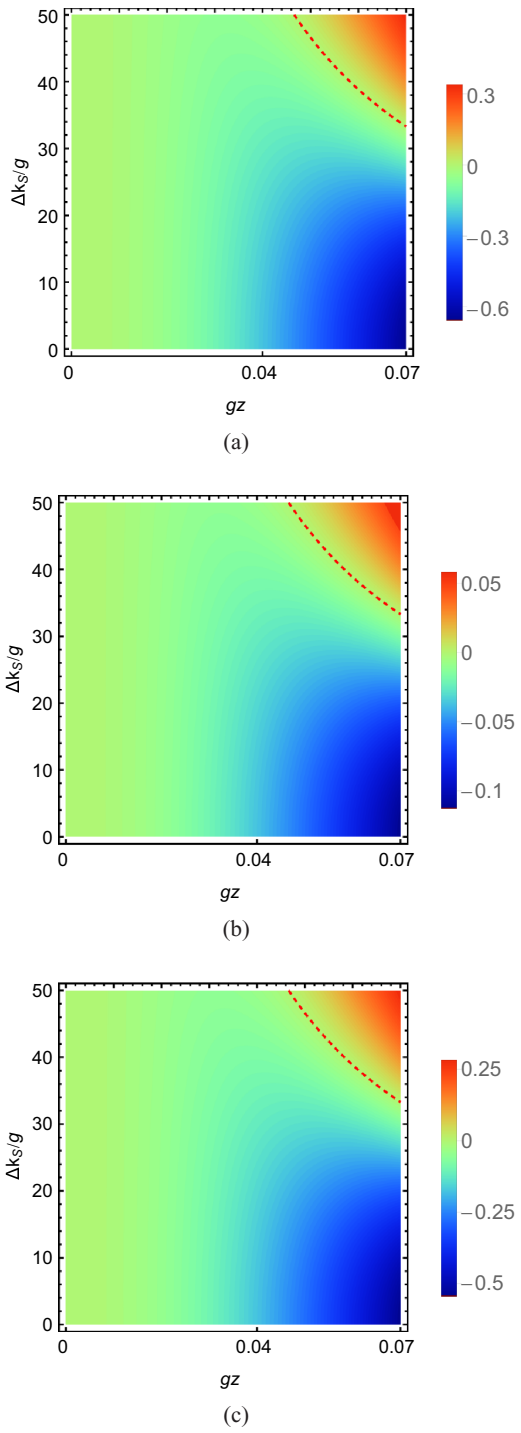

FIG. 4. Spatial evolution of Zeno parameter Z_j as a function of the phase mismatch parameter for (a) Stokes, (b) anti-Stokes, and (c) phonon modes considering both the phase difference parameters $\theta_i = 0$ with $\Delta k_D = 10^{-3} g$ and $\Delta k_A = \Delta k_S$. The rest of the parameters are the same as in the previous figure.

V. CONCLUSION

The dynamics of a nonlinear waveguide operating under the hyper-Raman process is obtained in terms of the spatial evolution of the photon and phonon numbers of the Stokes, anti-Stokes, and vibration modes. We subsequently consider

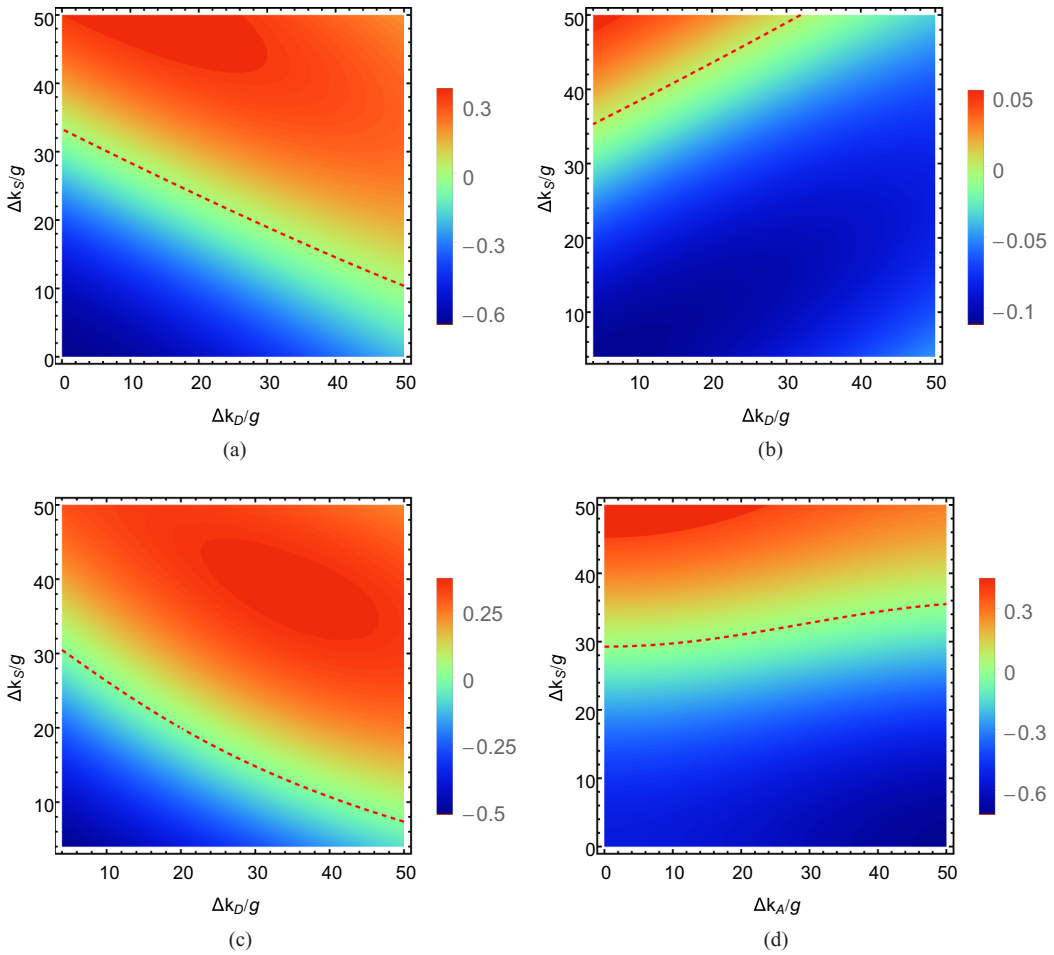

FIG. 5. Variation of Zeno parameters as a function of the phase mismatch parameters for (a) Stokes $Z_b(\Delta k_S, \Delta k_D)$, (b) anti-Stokes $Z_d(\Delta k_A = \Delta k_S, \Delta k_D)$, (c) phonon $Z_c(\Delta k_A = \Delta k_S, \Delta k_D)$, and (d) phonon $Z_c(\Delta k_S, \Delta k_A, \Delta k_D = 10^{-3}g)$ modes considering both phase difference parameters $\theta_i = 0$ and $gz = 0.07$. The rest of the parameters are the same as the previous figure.

that this waveguide (referred to as a system) is constantly gazed upon by a probe waveguide interacting with the nondegenerate pump modes of the hyper-Raman process. We obtain the dynamics of the system waveguide in this combined system-probe optical coupler in a completely quantum treatment by solving the Heisenberg's equations of motion for the corresponding momentum operator. These two cases allow us to quantify the effect of the presence of the probe waveguide on the system waveguide as the Zeno parameter. Specifically, if the presence of the probe is found to enhance (suppress) the generation of bosons in Stokes, anti-Stokes, and phonon modes it is referred to as QAZE (QZE).

The conservation of Stokes–anti-Stokes photon and phonon numbers is reflected in the relation between the Zeno parameters for the concerned modes. To be specific, the Zeno parameter for the phonon mode is the difference between that of the Stokes and anti-Stokes modes. The present study allows us to conclude that both QZE and QAZE disappear in spontaneous and some of the partially stimulated cases. Interestingly, the Zeno parameter depends on the intensities of pump, probe, and phonon modes as well as the system-probe coupling strength. However, none of these parameters can cause a crossover from QZE to QAZE and vice versa, as they always remain positive and thus can only alter the depth of the Zeno parameter. A similar effect was shown by the spatial evolution for the small values of the phase mismatch parameters.

Interestingly, the hyper-Raman based optical coupler in both cases with and without phase matching shows dependence on phase difference parameters in Stokes and anti-Stokes generation processes. Similarly, the phase mismatch parameters offer another set of control parameters to induce a transition between QZE and QAZE. In short, we have analytically obtained the solution of an interesting question: Which physical parameters control the dynamics of QZE and QAZE, and which of them can cause a transition from QZE to QAZE and vice versa?

Due to the general nature of the system under consideration, namely the nondegenerate hyper-Raman process, the obtained results can be reduced to corresponding Raman and degenerate hyper-Raman processes. Specifically, the dependence on all the parameters and the nature of the Zeno parameter in these special cases is expected to be similar to the present case with only a scaling factor. Further, the present study reveals that generation of nonclassical states can be controlled by introducing an auxiliary probe mode. For instance, for a suitable choice of phase difference parameters $\theta_1 = \theta_2 = \pi$ hyper-Raman scattering may lead to a larger Stokes

and anti-Stokes photon generation. In view of some recent results [49], this can be exploited to enhance generation of Stokes–anti-Stokes photon pairs in hyper-Raman scattering. We conclude the present work in hope that this work focused on a foundationally relevant topic will lead to applications in counterfactual quantum communication and computation as the physical system considered here and all its special cases are physically realizable using current technologies available in the domain of integrated optics as well as conventional bulk optics.

ACKNOWLEDGMENTS

A.P. acknowledges support from the Interdisciplinary Cyber Physical Systems (ICPS) program of the Department of Science and Technology (DST), India, Grant No. DST/ICPS/QuST/Theme-1/2019/14. K.T. acknowledges financial support from the Operational Programme Research, Development, and Education–European Regional Development Fund, Project No. CZ.02.1.01/0.0/0.0/16_019/0000754, of the Ministry of Education, Youth, and Sports of the Czech Republic.

APPENDIX A: MATHEMATICAL DETAILS OF THE SOLUTION

The Heisenberg's equations of motion for all six modes in the probe and system waveguides can be obtained as

$$\begin{aligned}
\dot{a}_p(z) &= i(k_p a_p + \Gamma a_1 a_2),\\
\dot{a}_1(z) &= i(k_{a_1} a_1 + g a_2^\dagger bc + \chi a_2^\dagger c^\dagger d + \Gamma a_p a_2^\dagger),\\
\dot{a}_2(z) &= i(k_{a_2} a_2 + g a_1^\dagger bc + \chi a_1^\dagger c^\dagger d + \Gamma a_p a_1^\dagger),\\
\dot{b}(z) &= i(k_b b + g a_1 a_2 c^\dagger),\\
\dot{c}(z) &= i(k_c c + g a_1 a_2 b^\dagger + \chi a_1^\dagger a_2^\dagger d),\\
\dot{d}(z) &= i(k_d d + \chi a_1 a_2 c).
\end{aligned} \tag{A1}$$

This set of coupled-operator differential equations is not exactly solvable in the closed analytic form. A perturbative solution of the coupled differential equations (A1) is obtained up to the quadratic terms in the interaction constants (g, χ, and Γ). Using the obtained spatial evolution of all the field and phonon modes in the closed analytic form, we obtain the number operators for Stokes, phonon, and anti-Stokes modes as

$$\begin{aligned}
\langle N_b\rangle = {} & |\beta|^2 + |j_2|^2|\alpha_1|^2|\alpha_2|^2(|\gamma|^2+1) + \big[\big\{j_1 j_2^\star \alpha_1^\star \alpha_2^\star \beta\gamma + j_1 j_3^\star \alpha_1^{\star 2}\alpha_2^{\star 2}\beta\delta + j_1 j_4^\star(|\alpha_1|^2+1)\beta\gamma^2\delta^\star\\
& + j_1 j_5^\star|\alpha_2|^2\beta\gamma^2\delta^\star + j_1 j_6^\star(|\alpha_1|^2+1)\alpha^\star\beta\gamma + j_1 j_7^\star|\alpha_2|^2\alpha^\star\beta\gamma + j_1 j_8^\star|\alpha_1|^2|\alpha_2|^2|\beta|^2 + j_1 j_9^\star|\beta|^2\\
& \times(|\alpha_1|^2+1)|\gamma|^2 + j_1 j_{10}^\star|\alpha_2|^2|\beta|^2|\gamma|^2 + \text{c.c.}\big\}\big],
\end{aligned} \tag{A2}$$

$$\begin{aligned}
\langle N_c\rangle = {} & |\gamma|^2 + |k_2|^2|\alpha_1|^2|\alpha_2|^2(|\beta|^2+1) + |k_3|^2(|\alpha_1|^2+1)(|\alpha_2|^2+1)|\delta|^2 + \big[\big\{k_1 k_2^\star \alpha_1^\star\alpha_2^\star\beta\gamma\\
& + k_1 k_3^\star \alpha_1\alpha_2\gamma\delta^\star + k_1 k_4^\star(|\alpha_1|^2+1)\alpha^\star\beta\gamma + k_1 k_5^\star|\alpha_2|^2\alpha^\star\beta\gamma + k_1 k_6^\star|\alpha_1|^2\alpha\gamma\delta^\star\\
& + k_1 k_7^\star(|\alpha_2|^2+1)\alpha\gamma\delta^\star + k_2 k_3^\star\alpha_1^2\alpha_2^2\beta^\star\delta^\star + k_1 k_8^\star|\alpha_1|^2|\alpha_2|^2|\gamma|^2 + k_1 k_9^\star(|\alpha_1|^2+1)\\
& \times|\beta|^2|\gamma|^2 + k_1 k_{10}^\star|\alpha_2|^2|\beta|^2|\gamma|^2 + k_1 k_{11}^\star|\alpha_1|^2|\gamma|^2|\delta|^2 + k_1 k_{12}^\star(|\alpha_2|^2+1)|\gamma|^2|\delta|^2\\
& + k_1 k_{13}^\star|\alpha_1|^2|\alpha_2|^2|\gamma|^2 + k_1 k_{14}^\star(|\alpha_1|^2+|\alpha_2|^2+1)\beta\gamma^2\delta^\star\big\} + \text{c.c.}\big],
\end{aligned} \tag{A3}$$

and

$$\begin{aligned}
\langle N_d\rangle = {} & |\delta|^2 + |l_2|^2|\alpha_1|^2|\alpha_2|^2|\gamma|^2 + \big[\big\{l_1 l_2^\star\alpha_1^\star\alpha_2^\star\gamma^\star\delta + l_1 l_3^\star(|\alpha_1|^2+1)\beta^\star\gamma^{\star 2}\delta + l_1 l_4^\star|\alpha_2|^2\beta^\star\gamma^{\star 2}\delta\\
& + l_1 l_5^\star\alpha_1^{\star 2}\alpha_2^{\star 2}\beta\delta + l_1 l_6^\star(|\alpha_1|^2+1)\alpha^\star\gamma^\star\delta + l_1 l_7^\star|\alpha_2|^2\alpha^\star\gamma^\star\delta + l_1 l_8^\star(|\alpha_1|^2+1)|\gamma|^2|\delta|^2\\
& + l_1 l_9^\star|\alpha_2|^2|\gamma|^2|\delta|^2 + l_1 l_{10}^*(|\alpha_1|^2+1)(|\alpha_2|^2+1)|\delta|^2\big\} + \text{c.c.}\big],
\end{aligned} \tag{A4}$$

respectively. The functional forms of coefficients of complex amplitude parameters are

$$\begin{aligned}
j_1 &= e^{iz k_b},\\
\frac{j_2}{j_1} &= \frac{g(1-e^{-iz\Delta k_S})}{\Delta k_S},\\
\frac{j_3}{j_1} &= \frac{g\chi(\Delta k_A - \Delta k_1 e^{-iz\Delta k_S} - \Delta k_S e^{iz\Delta k_1})}{\Delta k_A \Delta k_1 \Delta k_S},\\
\frac{j_4}{j_1} &= \frac{j_5}{j_1} = \frac{g\chi(\Delta k_A + \Delta k_S e^{-iz\Delta k_2} - \Delta k_2 e^{-iz\Delta k_S})}{\Delta k_A \Delta k_S \Delta k_2},\\
\frac{j_6}{j_1} &= \frac{j_7}{j_1} = \frac{g\Gamma(\Delta k_D + \Delta k_S e^{-iz\Delta k_3} - \Delta k_3 e^{-iz\Delta k_S})}{\Delta k_D \Delta k_S \Delta k_3},\\
\frac{j_8}{j_1} &= -\frac{j_9}{j_1} = -\frac{j_{10}}{j_1} = \frac{g^2(1-e^{-iz\Delta k_S} - i\Delta k_S z)}{\Delta k_S^2},
\end{aligned} \tag{A5}$$

$$
\begin{aligned}
k_1 &= e^{izk_c},\\
\frac{k_2}{k_1} &= \frac{g(1-e^{-iz\Delta k_S})}{\Delta k_S},\\
\frac{k_3}{k_1} &= \frac{\chi(1-e^{-iz\Delta k_A})}{\Delta k_A},\\
\frac{k_4}{k_1} &= \frac{k_5}{k_1} = \frac{g\Gamma(\Delta k_D + \Delta k_S e^{-iz\Delta k_3} - \Delta k_3 e^{-iz\Delta k_S})}{\Delta k_D \Delta k_S \Delta k_3},\\
\frac{k_6}{k_1} &= \frac{k_7}{k_1} = \frac{\Gamma\chi(-\Delta k_D + \Delta k_A e^{-iz\Delta k_4} - \Delta k_4 e^{-iz\Delta k_A})}{\Delta k_A \Delta k_D \Delta k_4},\\
\frac{k_8}{k_1} &= -\frac{k_{11}}{k_1} = -\frac{k_{12}}{k_1} = -\frac{\chi^2(1-e^{-iz\Delta k_A} - i\Delta k_A z)}{\Delta k_A^2},\\
\frac{k_9}{k_1} &= \frac{k_{10}}{k_1} = -\frac{k_{13}}{k_1} = -\frac{g^2(1-e^{iz\Delta k_S} - i\Delta k_S z)}{\Delta k_S^2},\\
\frac{k_{14}}{k_1} &= \frac{k_{15}}{k_1} = \frac{g\chi\{\Delta k_2(e^{-i\Delta k_A z} - e^{-i\Delta k_S z}) + \Delta k_1(1-e^{-i\Delta k_2 z})\}}{\Delta k_S \Delta k_A \Delta k_2},
\end{aligned}
\tag{A6}
$$

and

$$
\begin{aligned}
l_1 &= e^{izk_d},\\
\frac{l_2}{l_1} &= -\frac{\chi(1-e^{iz\Delta k_A})}{\Delta k_A},\\
\frac{l_3}{l_1} &= \frac{l_4}{l_1} = \frac{g\chi(\Delta k_S + \Delta k_A e^{iz\Delta k_2} - \Delta k_2 e^{iz\Delta k_A})}{\Delta k_S \Delta k_A \Delta k_2},\\
\frac{l_5}{l_1} &= \frac{g\chi(\Delta k_S + \Delta k_1 e^{iz\Delta k_A} - \Delta k_A e^{iz\Delta k_1})}{\Delta k_S \Delta k_1 \Delta k_A},\\
\frac{l_6}{l_1} &= \frac{l_7}{l_1} = \frac{\Gamma\chi(\Delta k_D - \Delta k_A e^{iz\Delta k_4} + \Delta k_4 e^{iz\Delta k_A})}{\Delta k_D \Delta k_A \Delta k_4},\\
\frac{l_8}{l_1} &= \frac{l_9}{l_1} = \frac{l_{10}}{l_1} = -\frac{\chi^2(1-e^{iz\Delta k_A} + i\Delta k_A z)}{\Delta k_A^2},
\end{aligned}
\tag{A7}
$$

where $\Delta k_S = (-k_{a_1} - k_{a_2} + k_b + k_c)$, $\Delta k_A = (k_{a_1} + k_{a_2} + k_c - k_d)$, $\Delta k_D = (k_{a_1} + k_{a_2} - k_p)$, $\Delta k_1 = \Delta k_A - \Delta k_S$, $\Delta k_2 = \Delta k_A + \Delta k_S$, $\Delta k_3 = \Delta k_S + \Delta k_D$, and $\Delta k_4 = \Delta k_A - \Delta k_D$.

APPENDIX B: DESCRIPTION OF PERTURBATIVE SOLUTION

The set of coupled differential equations (A1) involves nonlinear operators and thus these are not exactly solvable in the closed analytical form under the weak pump condition. In the Sen-Mandal perturbative technique, we assume the spatial evolution of an arbitrary mode in terms of the product of all the powers of the initial values of operators $A(z) = \sum_{i,j,k,l,m,n,o,p,q,r,s,t} \mathcal{F}_y a_p^{\dagger i}(0) a_p^j(0) a_1^{\dagger k}(0) a_1^l(0) a_2^{\dagger m}(0) a_2^n(0) \times b^{\dagger o}(0) b^p(0) c^{\dagger q}(0) c^r(0) d^{\dagger s}(0) d^t(0)$. However, this would be an infinite series which is truncated to include only $\mathcal{F}_y$ with not higher than quadratic terms in $\Lambda t\, \forall\, \Lambda \in \{g, \chi, \Gamma\}$. For instance, the assumed solution for Stokes mode is obtained as

$$
\begin{aligned}
b(z) = {} & j_1 b(0) + j_2 a_1(0) a_2(0) c^\dagger(0) + j_3 a_1^2(0) a_2^2(0) d^\dagger(0)\\
& + j_4 a_1(0) a_1^\dagger(0) c^{\dagger 2}(0) d(0) + j_5 a_2^\dagger(0) a_2(0) c^{\dagger 2}(0) d(0)\\
& + j_6 a_p(0) a_1(0) a_1^\dagger(0) c^\dagger(0) + j_7 a_p(0) a_2^\dagger(0) a_2(0) c^\dagger(0)\\
& + j_8 a_1^\dagger(0) a_1(0) a_2^\dagger(0) a_2(0) b(0) + j_9 a_1(0) a_1^\dagger(0) b(0)\\
& \times c^\dagger(0) c(0) + j_{10} a_2^\dagger(0) a_2(0) b(0) c^\dagger(0) c(0).
\end{aligned}
\tag{B1}
$$

To obtain all the coefficients j_n we use the fact that the spatial evolution of the Stokes mode $b(z)$ is defined as

$$
\begin{aligned}
b(z) &= e^{iGz} b(0) e^{-iGz}\\
&= b(0) + iz[G, b] + \frac{(iz)^2}{2!}[G, [G, b]] + \ldots,
\end{aligned}
\tag{B2}
$$

where all the nested commutators are obtained as

$$
[G, b] = -(k_b b + g a_1 a_2 c^\dagger) \tag{B3}
$$

and

$$
\begin{aligned}
[G, [G, b]] = {} & k_b^2 b + g\big(k_{a_1} + k_{a_2} + k_b - k_c\big)\\
& \times a_1 a_2 c^\dagger - g\chi\big(a_1^2 a_2^2 d^\dagger - a_1 a_1^\dagger c^{\dagger 2} d - a_2^\dagger a_2 c^{\dagger 2} d\big)\\
& + g\Gamma(a_p a_1 a_1^\dagger c^\dagger + a_p a_2^\dagger a_2 c^\dagger)\\
& - g^2(a_1^\dagger a_1 a_2^\dagger a_2 b - a_1 a_1^\dagger b c^\dagger c - a_2^\dagger a_2 b c^\dagger c),
\end{aligned}
\tag{B4}
$$

etc., ignoring all the terms beyond the quadratic powers of the interaction constants g, χ, and Γ. We use all the functions of operators occurring in the higher-order nested commutators with unknown coefficients j_n. From the set of assumed solution for the spatial evolution all the operators we obtain a set of coupled differential equations of all the coefficients $\mathcal{F}_y$ using Eq. (B1) in Eq. (A1), as

$$
\begin{aligned}
\dot{j}_1(z) &= ik_b j_1,\\
\dot{j}_2(z) &= i(k_b j_2 + g g_1 h_1 k_1^\star),\\
\dot{j}_3(z) &= i(k_b j_3 + g g_1 h_1 k_3^\star),\\
\dot{j}_4(z) &= i(k_b j_4 + g g_1 h_3 k_1^\star),\\
\dot{j}_5(z) &= i(k_b j_5 + g g_3 h_1 k_1^\star),\\
\dot{j}_6(z) &= i(k_b j_6 + g g_1 h_4 k_1^\star),\\
\dot{j}_7(z) &= i(k_b j_7 + g g_4 h_1 k_1^\star),\\
\dot{j}_8(z) &= i(k_b j_8 + g g_1 h_1 k_2^\star),\\
\dot{j}_9(z) &= i(k_b j_9 + g g_1 h_2 k_1^\star),\\
\dot{j}_{10}(z) &= i(k_b j_{10} + g g_2 h_1 k_1^\star).
\end{aligned}
\tag{B5}
$$

The solution of coupled differential equations of $\mathcal{F}_y$ with initial conditions $\mathcal{F}_y = \delta_{y,1}$ at $t = 0$ gives us the analytical form of j_n (and other $\mathcal{F}_y$) reported in Eq. (A5).

Here, it will be apt to note that in a strict sense, the validity of the short-length solution [51] is limited by $|\Lambda z \xi| < 1$, where $\Lambda = \max\{g, \chi, \Gamma\}$ and $\xi = \max \xi\, \forall \xi \in$

$\{\alpha, \alpha_1, \alpha_2, \beta, \gamma, \delta\}$. This gives us the validity of the short-length solution for propagation lengths $z < 1/|\Lambda\xi|$, while the present perturbative solution has enlarged validity for finite times due to modulation by the sinc function related to the phase mismatches, which ensures the convergence (see [43] for details).

[1] B. Misra and E. C. G. Sudarshan, J. Math. Phys. **18**, 756 (1977).
[2] L. A. Khalfin, Dokl. Akad. Nauk SSSR **115**, 277 (1957) [Sov. Phys. Dokl. **2**, 232 (1958)]; Zh. Eksp. Teor. Fiz. **33**, 1371 (1958) [Sov. Phys. JETP **6**, 1053 (1958)]; Dokl. Akad. Nauk SSSR **141**, 599 (1961) [Sov. Phys. Dokl. **6**, 1010 (1962)].
[3] A. Venugopalan, Resonance **12**, 52 (2007).
[4] P. Facchi and S. Pascazio, in *Quantum Zeno and Inverse Quantum Zeno Effects*, edited by E. Wolf, Progress in Optics, Vol. 42 (Elsevier, Amsterdam, 2001), pp. 147–218.
[5] S. Pascazio, Open Systems and Information Dynamics **21**, 1440007 (2014).
[6] K. Thapliyal and A. Pathak, Proc. SPIE **9654**, 96541F1 (2015).
[7] J. Naikoo, K. Thapliyal, S. Banerjee, and A. Pathak, Phys. Rev. A **99**, 023820 (2019).
[8] K. Thapliyal, A. Pathak, and J. Peřina, Phys. Rev. A **93**, 022107 (2016).
[9] P. Facchi and S. Pascazio, in *Irreversible Quantum Dynamics*, edited by F. Benatti and R. Floreanini, Lecture Notes in Physics Vol. 622 (Springer, Berlin, Heidelberg, 2003), p. 141.
[10] K. Kraus, Found. Phys. **11**, 547 (1981).
[11] L. S. Schulman, Phys. Rev. A **57**, 1509 (1998).
[12] P. Facchi, D. A. Lidar, and S. Pascazio, Phys. Rev. A **69**, 032314 (2004).
[13] J. M. Zhang, J. Jing, L. G. Wang, and S. Y. Zhu, Phys. Rev. A **98**, 012135 (2018).
[14] K. Thun, J. Peřina, and J. Křepelka, Phys. Lett. A **299**, 19 (2002).
[15] J. Řeháček, J. Peřina, P. Facchi, S. Pascazio, and L. Mišta Jr., Opt. Spectrosc. **91**, 501 (2001).
[16] L. Mišta Jr., V. Jelínek, J. Rehácek, and J. Peřina, J. Opt. B: Quantum Semiclassical Opt. **2**, 726 (2000).
[17] J. Řeháček, J. Peřina, P. Facchi, S. Pascazio, and L. Mišta, Phys. Rev. A **62**, 013804 (2000).
[18] A. Luis and J. Peřina, Phys. Rev. Lett. **76**, 4340 (1996).
[19] A. Luis and L. L. Sánchez-Soto, Phys. Rev. A **57**, 781 (1998).
[20] J. Peřina, Phys. Lett. A **325**, 16 (2004).
[21] G. S. Agarwal and S. P. Tewari, Phys. Lett. A **185**, 139 (1994).
[22] J. C. F. Matthews, A. Politi, A. Stefanov, and J. L. O'Brien, Nat. Photonics **3**, 346 (2009).
[23] S. Tanzilli, A. Martin, F. Kaiser, M. P. De Micheli, O. Alibart, and D. B. Ostrowsky, Laser Photonics Rev. **6**, 115 (2012).
[24] K. Thapliyal, A. Pathak, B. Sen, and J. Peřina, Phys. Rev. A **90**, 013808 (2014).
[25] P. G. Kwiat, A. G. White, J. R. Mitchell, O. Nairz, G. Weihs, H. Weinfurter, and A. Zeilinger, Phys. Rev. Lett. **83**, 4725 (1999).
[26] W. M. Itano, D. J. Heinzen, J. J. Bollinger, and D. J. Wineland, Phys. Rev. A **41**, 2295 (1990).
[27] M. C. Fischer, B. Gutiérrez-Medina, and M. G. Raizen, Phys. Rev. Lett. **87**, 040402 (2001).
[28] O. Hosten, M. T. Rakher, J. T. Barreiro, N. A. Peters, and P. G. Kwiat, Nature (London) **439**, 949 (2006).
[29] H. Salih, Z. H. Li, M. Al-Amri, and M. S. Zubairy, Phys. Rev. Lett. **110**, 170502 (2013).
[30] P. Facchi, Z. Hradil, G. Krenn, S. Pascazio, and J. Řeháček, Phys. Rev. A **66**, 012110 (2002).
[31] S. Pascazio, P. Facchi, Z. Hradil, G. Krenn, and J. Rehacek, Fortschr. Phys. **49**, 1071 (2001).
[32] A. Tavakoli, H. Anwer, A. Hameedi, and M. Bourennane, Phys. Rev. A **92**, 012303 (2015).
[33] A. Beige, D. Braun, B. Tregenna, and P. L. Knight, Phys. Rev. Lett. **85**, 1762 (2000).
[34] Y. Cao, Y.-H. Li, Z. Cao, J. Yin, Y.-A. Chen, H.-L. Yin, T.-Y. Chen, X. Ma, C.-Z. Peng, and J.-W. Pan, Proc. Natl. Acad. Sci. **114**, 4920 (2017).
[35] H. Nikolić, Phys. Lett. B **733**, 6 (2014).
[36] D. A. Zezyulin, V. V. Konotop, G. Barontini, and H. Ott, Phys. Rev. Lett. **109**, 020405 (2012).
[37] J. L. O'Brien, A. Furusawa, and J. Vučković, Nat. Photonics **3**, 687 (2009).
[38] A. Politi, M. J. Cryan, J. G. Rarity, S. Yu, and J. L. O'Brien, Science **320**, 646 (2008).
[39] K. Thapliyal, A. Pathak, B. Sen, and J. Peřina, Phys. Lett. A **378**, 3431 (2014).
[40] B. Sen and S. Mandal, J. Mod. Opt. **52**, 1789 (2005).
[41] S. Mandal and J. Peřina, Phys. Lett. A **328**, 144 (2004).
[42] J. Peřina, *Quantum Statistics of Linear and Nonlinear Optical Phenomena* (Kluwer Academic, Dordrecht, 1991).
[43] K. Thapliyal and J. Peřina, Phys. Lett. A **383**, 2011 (2019).
[44] K. Thapliyal and J. Peřina, Phys. Scr. **95**, 034001 (2020).
[45] S. Dochow, M. Becker, R. Spittel, C. Beleites, S. Stanca, I. Latka, K. Schuster *et al.*, Lab Chip **13**, 1109 (2013).
[46] A. Dhakal, F. Peyskens, S. Clemmen, A. Raza, P. Wuytens, H. Zhao, N. L. Thomas, and R. Baets, Interface Focus **6**, 20160015 (2016).
[47] F. Madzharova, Z. Heiner, J. Simke, S. Selve, and J. Kneipp, J. Phys. Chem. C **122**, 2931 (2018).
[48] R. Tan, D. F. Kelley, and A. M. Kelley, J. Phys. Chem. C **123**, 16400 (2019).
[49] M. Kasperczyk, F. S. de Aguiar Júnior, C. Rabelo, A. Saraiva, M. F. Santos, L. Novotny, and A. Jorio, Phys. Rev. Lett. **117**, 243603 (2016).
[50] L.-M. Duan, M. D. Lukin, J. I. Cirac, and P. Zoller, Nature (London) **414**, 413 (2001).
[51] V. Peřinová and J. Peřina, Czechoslov. J. Phys. B **28**, 1183 (1978).